Motion Tolerant Magnetic Earring Sensor and Wireless Earpiece for Wearable Photoplethysmography

Ming-Zher Poh, *Student Member, IEEE,* Nicholas C. Swenson, and Rosalind W. Picard, *Fellow, IEEE*

***Abstract*— This paper addresses the design considerations and critical evaluation of a novel embodiment for wearable photoplethysmography (PPG) comprising a magnetic earring sensor and wireless earpiece. The miniaturized sensor can be worn comfortably on the earlobe and contains an embedded accelerometer to provide motion reference for adaptive noise cancellation. The compact wireless earpiece provides analog signal conditioning and acts as a data-forwarding device via a radio frequency transceiver. Using Bland-Altman and correlation analysis, we evaluated the performance of the proposed system against an FDA-approved electrocardiogram (ECG) measurement device during daily activities. The mean ± SD of the differences between heart rate measurements from the proposed device and ECG (expressed as percentage of the average between the two techniques) along with the 95% limits of agreement (LOA = ± 1.96 SD) was 0.62 ± 4.51% (LOA = -8.23 and 9.46%), -0.49 ± 8.65% (-17.39 and 16.42%) and -0.32 ± 10.63% (-21.15 and 20.52%) during standing, walking and running respectively. Linear regression indicated a high correlation between the two measurements across the three evaluated conditions (r = 0.97, 0.82 and 0.76 respectively with p < 0.001). The new earring PPG system provides a platform for comfortable, robust, unobtrusive and discreet monitoring of cardiovascular function.**

***Index Terms*— photoplethysmography (PPG), heart rate, motion noise removal, wearable biosensors, ambulatory monitoring, pervasive health**

I. Introduction

Wearable biosensors have the potential to revolutionize healthcare by realizing low-cost and pervasive physiological monitoring. Continuous and non-invasive assessments of cardiovascular function are important in promoting healthy lifestyles, surveillance for cardiovascular catastrophes and assessing the impact of clinical interventions [1]. By enabling comfortable and continuous cardiovascular monitoring outside of a clinical setting over extended periods of time, wearable biosensors could play an important role in many areas, ranging from personal health monitoring to sports medicine and hazardous operations. For example, remote and unobtrusive monitoring of vital signs from emergency operators such as firefighters, military combatants, law enforcement officers or paramedics operating in harsh and hazardous environments would allow early identification of injuries sustained. Timely intervention would reduce the fatality rate. During high-risk operations, continuous assessment of the fitness conditions of emergency operators could indicate their state of readiness for action and identify individuals that need to be relieved from duty. As such, wearable devices that track physiological information can assist emergency operators in making critical decisions and expedite rescue missions.

Photoplethysmography (PPG), in particular, can provide valuable information about the cardiovascular system such as heart rate, arterial blood oxygen saturation, blood pressure, cardiac output and autonomic function [2, 3] and is especially suitable for wearable sensing. This electro-optic technique of measuring the cardiovascular pulse waveform that propagates through the body has become increasingly popular due to its low cost and non-invasive means of sensing without the need for electrodes. Despite the attractive attributes of PPG and the ease of its integration into wearable devices, PPG is known to be susceptive to motion-induced signal corruption [4] and overcoming motion artifacts presents one of the most challenging problems. In most cases, the noise falls within the same frequency band as the physiological signal of interest, thus rendering linear filtering with fixed cut-off frequencies ineffective. Among the numerous signal processing techniques for minimizing motion artifacts in PPG signals explored [5-9], one of the most appealing methods is adaptive noise cancellation using accelerometers as a noise reference [10-14]. This technique introduced by Widrow *et al.* [15] provides a tool for estimating signals corrupted by additive noise and is capable of removing in-band disturbances and rapidly adjusting to changes in sensor attachment or system variations.

For wearable devices to be practical and effective in the field, careful design and placement of the sensors are also important to reduce the influence of motion artifacts sources. In addition to being unobtrusive and comfortable to wear, such devices have to be lightweight, robust and provide reliable sensor attachment. Ambulatory electrocardiogram (ECG)

Manuscript received July 21, 2009; revised November 24, 2009. This work was supported by the Nancy Lurie Marks Family Foundation (NLMFF).
M. Z. Poh is with the Harvard-MIT Division of Health Sciences and Technology (HST) and also with the Media Laboratory, Massachusetts Institute of Technology, Cambridge, MA 02139 USA (e-mail: zher@mit.edu).
N. C. Swenson is with the Media Laboratory, Massachusetts Institute of Technology, Cambridge, MA 02139 USA. (e-mail: nswenson@mit.edu).
R. W. Picard is a professor at the Media Laboratory, Massachusetts Institute of Technology, Cambridge, MA 02139 USA. (phone: 617-253-0611; fax: 617.253.5922; e-mail: picard@media.mit.edu).

devices can be uncomfortable, hinder motion and interfere with duties due to the cumbersome wires and adhesive electrode patches. Commercial PPG sensors that attach to the fingertips or earlobes are inconvenient for users and the ear-clip can cause pain if worn over a long period of time. As such, alternative measurement sites for wearable PPG sensing have been described, including the ring finger [4], forehead [16], wrist [5], external ear cartilage [17] and the superior auricular region [18]. Among these different measurement sites, the earlobe remains an attractive choice because it has a rich arterial supply [19] and is less affected by motion than other extremities. Despite earlobe plethysmography being an excellent source for pulse rate measurements [20], there has been a lack of development for wearable earlobe PPG sensors beyond the conventional spring-loaded earclip. One possible reason might be the stringent design requirements and space limits due to the ergonomics of an earlobe probe – all the sensing components need to fit into a compact package that is light and comfortable. There is also a need for a fully integrated, self-contain earpiece that has all the signal-conditioning circuitry, data acquisition and control electronics, wireless transceiver and battery embedded within. To our knowledge, all the existing ear-worn PPG systems require connections to external circuitry (many of which are commercial data acquisition hardware that was not designed to be wearable) and cannot function as an independent unit (Table 1a). The simplicity of a single earpiece reduces the number of items the wearer needs to put on and does not encumber the wearer, unlike the previous works that require wired connections to additional circuitry. This is especially important for emergency operators who typically already have to carry a lot of different equipment and cannot afford to be hampered while on the job.

In this work, we rethink and redesign the earlobe PPG sensor for wearable monitoring to meet these challenges. We propose a novel embodiment comprising a miniaturized magnetic earring PPG sensor and wireless earpiece that is compact, comfortable, unobtrusive and integrated with adaptive noise cancellation for motion artifact reduction. Section II illustrates the design and construction of the proposed earring sensor and wireless earpiece. Section III describes the experimental and analysis methods for validating the performance of the proposed system with an FDA-approved ECG device in heart rate estimation. The results from systematic evaluations during three common kinds of physical activities (standing, walking and running) are presented in Section IV. These activities are frequently performed by emergency operators, running in particular. Finally, we discuss our findings and further improvements to the proposed design for pervasive cardiovascular monitoring.

II. System Design

A. Construction of the Earring Sensor

The earring sensor is a miniaturized, unobtrusive device designed to measure the pulsation of blood flow in the vessels

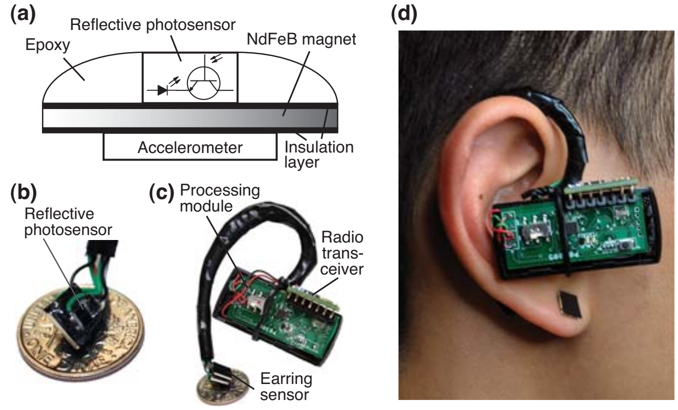

Fig. 1. Overview of the wearable system. (a) Schematic of the earring sensor. (b) Prototype of earring sensor showing an embedded reflective photosensor. An accelerometer (not visible) is embedded on the opposite side. (c) Packaging of the magnetic earring sensor and the wireless earpiece containing a processing module and radio transceiver. (d) Appearance of device when worn by user.

of the earlobe as well as motion of the ear. Fig. 1a shows the schematic of the earring sensor. The device consists of a nickel plated neodymium magnet measuring 6.4 mm × 6.4 mm × 0.8 mm that is insulated with electrical tape on both sides and serves as the substrate for mounting a reflective photosensor (CNB10112 by Panasonic) on one side and a three-axis accelerometer (ADXL330, Analog Devices) on the other. The reflective photosensor comprises a phototransistor and an infrared LED (peak emission wavelength at 940 nm) in a single package. A layer of epoxy was applied around the reflective photosensor to protect the wire connections and stabilize the photosensor.

The earring sensor can be worn against one side of the earlobe by attaching another neodymium magnet to the opposite side. Neodymium magnets are strong enough to hold the sensor in place even in the presence of motion. The reflective photosensor shines an IR light into the earlobe and measures the amount of light reflected from the subcutaneous blood vessels. During the cardiac cycle, volumetric changes in the blood vessels modify the path length of the incident light such that the subsequent changes in amount of reflected light indicate the timing of cardiovascular events. A more detailed review on the principles of PPG technology can be found in [2]. In general, the pulsatile amplitude of the PPG waveform increases with higher pressure induced by the magnetic earring sensor [21]. However, the amplitude will decrease as the pressure increases further due to obstruction of the superficial blood flow within the proximal subcutaneous capillaries, leading to insufficient blood perfusion [18]. Although powerful, the magnets do not cause pain by applying excessive pressure on the earlobe unlike conventional ear clips. The implemented earring sensor prototype with the embedded reflective photosensor (Fig. 1b) and accelerometer is very small and provides a promising means for comfortable and discreet monitoring of vital signs.

TABLE I
COMPARISON OF EAR-WORN PHOTOPLETHYSMOGRAPHY SYSTEMS

A. KEY FEATURES

Features	**New MIT Sensor**	Samsung [22]	Pulsear (CSEM) [17]	e-AR [18]	IN-MONIT [3, 23, 24]	CUHK [25]	Imperial College [26]
Sensing location	**Ear lobe**	**Ear lobe**	External ear cartilage	Superior auricle	Auditory canal	Inferior auricle	Superior auricle
Probe attachment	**Magnetic earring**	Spring-loaded clip	Earcup headphones	Earhook	Otoplastic insertion	Earhook	Tape
Fully integrated, self-contained earpiece*	**Yes**	No, needs external device for power	No, needs external circuitry and off-body DAQ hardware	No, needs external circuitry and off-body DAQ hardware	No, needs external circuitry (off-body)	No, needs external circuitry (neck-worn)	No, needs external circuitry and off-body DAQ hardware
Wireless communication	**Yes**	No	No	No	**Yes**	**Yes**	No
Motion cancellation	**ANC** (7 taps)	**ANC** (32 taps)	Principle component analysis	Passive motion cancellation	None	None	None

B. PERFORMANCE EVALUATION COMPLETED

Features	**New MIT Sensor**	Samsung [22]	Pulsear (CSEM) [17]	e-AR [18]	IN-MONIT [3, 23, 24]	CUHK [25]	Imperial College [26]
Evaluation at rest	**Yes**	**Yes**	**Yes**	**Yes**	**Yes**	**Yes**	No
Reference	**ECG**	**ECG**	**ECG**	Pulse ox.	Pulse ox.	Pulse ox.	-
Bland-Altman†	**Yes**	No	No	No	Yes	Yes	-
Walking test	**Yes**	**Yes**	**Yes**	Yes	Yes	No	No
Reference	**ECG**	**ECG**	**ECG**	Pulse ox.	Pulse ox.	-	-
Bland-Altman	**Yes**	No	No	No	No	-	-
Running test	**Yes**	**Yes**	**Yes**	No	No	No	No
Reference	**ECG**	**ECG**	**ECG**	-	-	-	-
Bland-Altman	**Yes**	No	No	-	-	-	-

*****Containing signal-conditioning circuitry, data acquisition/control electronics, wireless transceiver and battery.
†Standard method of statistical analysis for comparing a new clinical measurement technique with a gold standard [27].

B. Description of the Circuitry

Fig. 2 shows the system architecture of the proposed system. Two diodes in series convert the changes in phototransistor current from the earring sensor to a logarithmic voltage change to achieve a wide dynamic range of current measurements. The resulting output is passed through a four-stage active bandpass filter (0.8 – 4.0 Hz) to separate the ac component of the signal, reduce electrical noise as well as motion artifacts. The signals from the three-axis accelerometer are filtered with a simple RC circuit with a cutoff frequency of 5 Hz. A digital signal controller (DSC, dsPIC30F2012 by Microchip Technology, Inc.) was selected as the control unit because of its capability for performing complex analysis and signal processing on-board. The analog signals are sampled at 400 Hz via an A-D with 12-bit resolution on the DSC. The digital signals are then transmitted wirelessly to a laptop through the use of a pair of 2.4 GHz radio transceivers modules (nRF2401A by Sparkfun Electronics). Alternatively, the data can be sent to a handheld device such as a cellphone or personal digital assistant (PDA). A step-up/step-down charge pump (LTC3240 by Linear Technology) regulates a single lithium polymer battery (nominal voltage of 3.7 V) to produce a fixed output of 3.3 V for the DSC and peripheral components. The battery can be recharged from a USB port by an on-board single cell Li-Ion battery charger (LTC4062 by Linear Technology). The dimensions of the PCB containing the control/processing module are 15 mm × 35 mm × 0.8 mm.

C. Packaging

The processing unit was designed to fit into a standard Bluetooth wireless earpiece. This configuration is a rational design choice given the increasing popularity and acceptance of these communication devices. In particular, it is not uncommon for emergency operators such as firefighters, law enforcement officers, pilots and paramedics to wear communication earpieces while at work, thus this approach integrates mobile health monitoring into an item that is already familiar to them. Fig. 1c shows a prototype of the integrated system comprising the wireless earpiece and magnetic earring sensor. The electronics inside a Bluetooth earpiece (MINI-2PK, Nolan Systems) were removed and replaced by the proposed processing module. The outputs of the earring sensor were connected to the processing module by flexible wires running along the earhook and covered with electrical tape to provide a concealed interface. Fig 1d shows a close-up of the complete system worn by a user. With further packaging to conceal the electronics, the user would essentially appear to be wearing a standard Bluetooth earpiece and a magnetic earring. Hence, this design is favorable for non-stigmatizing and discreet health monitoring.

D. Adaptive Noise Cancellation

For any device to be truly wearable, it has to be able to tolerate motion artifacts generated when the user is on the move. While the intelligent design of sensor attachment, form factor and packaging can help reduce the impact of motion disturbances, it is rarely sufficient for noise removal.

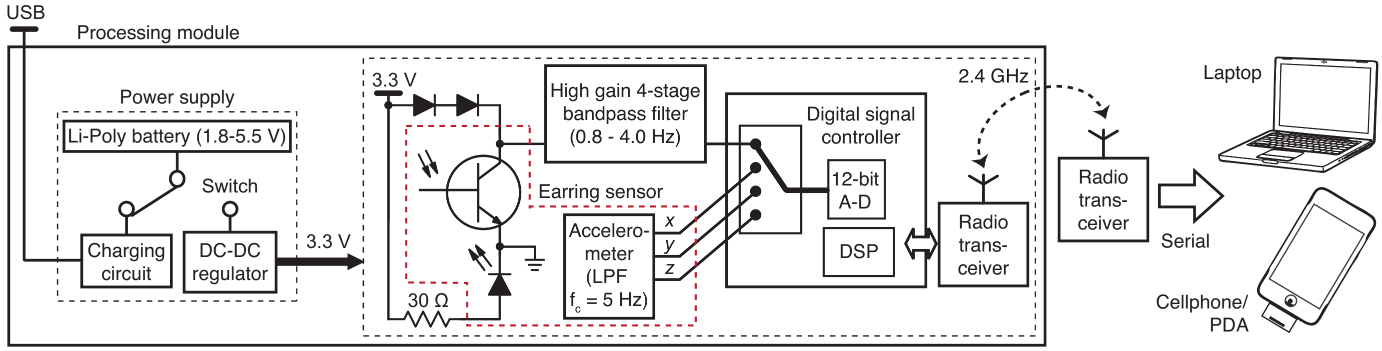

Fig. 2. Overview of the integrated system architecture.

Advanced signal processing techniques are often required to deal with motion artifacts under vigorous activity. As such, we adopted Widrow's Adaptive Noise Cancellation (ANC) to minimize motion artifacts in the proposed sensor. Fig. 3 shows the ANC configuration we utilized. The output of the PPG sensor y is a combination of the desired physiological signal of blood volume changes x, and a motion-induced noise signal m which are assumed to be additive. If the motion-induced noise signal is known, the desired (but unknown) physiological signal can then be recovered by subtracting the motion artifacts from the corrupted output of the PPG sensor. It is possible that the linearity is not representative of the true contribution of motion to the PPG signal given that the reflected light intensity varies nonlinearly with distance traveled through the ear according to the Beer-Lambert law. In addition, the physiological changes in blood volume due to motion are not well understood and could also be nonlinear. Nonetheless, since the filter coefficients are adaptively computed, a linear model should provide a reasonable local approximation for the motion-to-noise relationship [28].

The actual motion experienced by the PPG sensor is measured by the vertical axis of the accelerometer and serves as a noise reference input that is correlated to the motion-induced noise signal. This reference input is then processed by an adaptive filter that continuously readjusts its impulse response in response to an error signal that is dependent, among other things, on the dynamic input signal and filter's output to produce $\hat{m}$, an estimation of the motion-induced noise signal. The system output $\hat{x} = y - \hat{m}$, in addition to providing the recovered signal, also feeds back to the adaptive filter as an error signal.

By assuming that the desired signal x is not correlated with the motion-induced noise signal m or its estimate $\hat{m}$, it can be shown [15] that when the filter is adjusted such that the power of the system output $E[\hat{x}^2]$ is minimized, $E[(m-\hat{m})^2]$ is also minimized and thus causes the recovered signal $\hat{x}$ to be a best least squares estimate of the desired signal x. Using an FIR model for the filter, the process parameters to identify are the filter coefficients that produce the estimate of the motion-induced noise signal $\hat{m}$:

$$\hat{m}_t = \boldsymbol{h}_t^T \cdot \boldsymbol{a}_t \tag{1}$$

where $\boldsymbol{h}_t = [h_1, h_2, ..., h_n]^T$

$$\boldsymbol{a}_t = [a_t, a_{t-1}, ..., a_{t-n+1}]^T$$

Here $\boldsymbol{h}_t$ is the filter coefficient vector estimated at time t, h_i represents the i^{th} FIR filter coefficient, n is the model order and the input vector $\boldsymbol{a}_t$ consists of a time sequence of measured acceleration a.

We utilized the standard least mean-square (LMS) algorithm to adaptively minimize the signal power for the filter coefficient estimations. The LMS algorithm update of the filter coefficient vector with a step size of μ is given by:

$$\boldsymbol{h}_{t+1} = \boldsymbol{h}_t + \mu \hat{x}_t \boldsymbol{a}_t \tag{2}$$

Keeping the trade-off between algorithm complexity and computation time in mind, we selected filter model order of 7 and step size of 0.2. These design parameters were selected such that future work would allow for real-time computation by the DSC.

III. Experimental Methods

A. Study Description

We evaluated the performance of the new integrated system (earring sensor and wireless earpiece) against the established ECG method during three kinds of common physical activities (standing, walking and running). Fourteen participants (seven male, seven female) between the ages of 18-35 years were enrolled for this study that was approved by the Massachusetts Institute of Technology Committee On the Use of Humans as Experimental Subjects (COUHES). Informed consent was obtained from all the participants prior to the start of each study session. In addition to wearing the sensor earring and wireless earpiece, participants wore three adhesive electrodes on their chest to record ECG simultaneously. For all experiments, an FDA-approved and commercially available system (Flexcomp Infiniti by Thought Technologies Ltd.) was used to measure ECG at sampling rate of 256 Hz. The raw PPG and acceleration waveform from the earring sensor were transmitted wirelessly at 50 Hz to a receiver connected to a laptop for data recording.

Participants were asked to stand at rest on a treadmill (Precor USA, Inc.) for two minutes and then walk for one

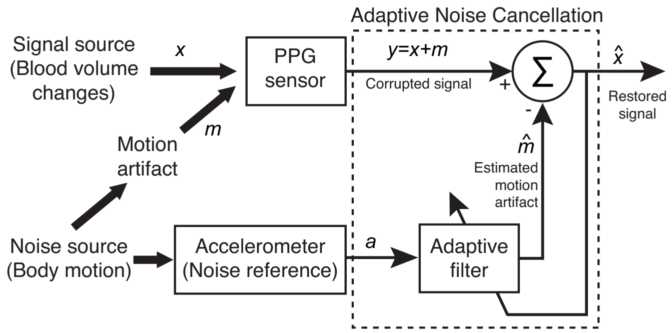

Fig. 3. Block diagram of adaptive noise cancellation (ANC) configuration.

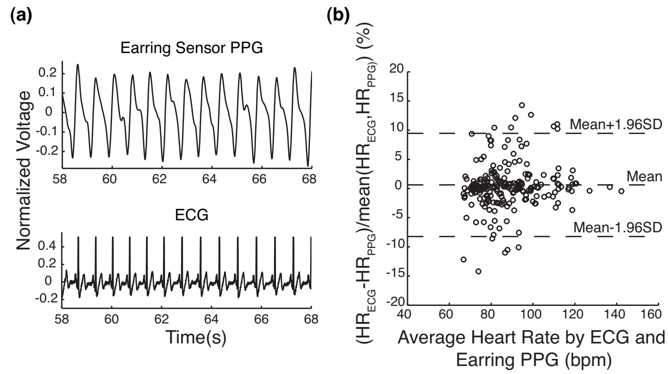

Fig. 4. (a) Comparison of a 10 s PPG waveform acquired from the earring sensor during standing with reference ECG. (b) Bland-Altman plot demonstrating the agreement between 15 s epoch heart rate measurements from the earring sensor and ECG during standing (a total of 218 measurement pairs from 14 subjects). The lines represent the mean and 95% limits of agreement.

minute during each increment of speed (3.2, 4.0, 4.8 and 5.6 km/h). This was followed by a three-minute period of standing at rest before participants were asked to run at 6.4 km/h for one minute then at 8.0 km/h for another minute before completing the experiment by standing at rest for two more minutes. We excluded data during the running session from one participant who declined to run and from another participant due to corrupted Flexcomp Infiniti ECG recordings.

B. Data Analysis and Statistics

Post processing and analysis of the recordings were done using custom software written in MATLAB (The MathWorks, Inc.). Both PPG and acceleration recordings were filtered with a 5-point moving average filter to remove outliers, upsampled from 50 Hz to 256 Hz using cubic spline interpolation. To allow for easier comparison and provide zero-mean signals for adaptive filtering, all signals were normalized using the following equation:

$$s_{normalized} = \frac{s - \bar{s}}{\max(s) - \min(s)} \tag{3}$$

The acceleration signal was then processed with a 1024-point highpass filter (Hamming window, cutoff frequency of 1 Hz) to remove the baseline trend. ANC was implemented with a 7th order FIR filter using the filtered acceleration signal as its input. The standard LMS algorithm with a step size of 0.2 was utilized to determine the filter coefficients. The output of the system was filtered with a 1024-point lowpass filter (Hamming window, cutoff frequency of 4 Hz) before performing peak detection. The PPG peak detection algorithm employed a variable amplitude threshold as well as a time threshold (minimum interbeat interval) to avoid false peak detections. RR intervals of the ECG signal were extracted using the QRS detection algorithm developed by Zhang *et al.* [29]. The resulting interbeat intervals derived from our system and the ECG signal were resampled to 10 Hz and average heart rate measurements were calculated over 15 s epochs with no overlap.

Bland Altman plots were used for combined graphical and statistical interpretation of the two measurement techniques. The differences between heart rate measurements from the earring sensor and ECG were expressed as percentage of the averages of both techniques and plotted against the averages. The mean and standard deviation (SD) of the differences, mean of the absolute differences and 95% limits of agreement were calculated. Pearson's correlation coefficients and the corresponding p-values were calculated for the estimated heart rate from the proposed device and ECG.

IV. Results

A. Earring PPG and ECG Measurements During Standing Show High Agreement

All the participants reported that the earring sensor and wireless earpiece felt comfortable. Given that the wireless earpiece had a fixed-sized earhook (presumably designed to fit the average ear size), the quality of fit of the wireless earpiece depended on the size of the participant's ear. Nonetheless, both the earpiece and earring sensor stayed on throughout all the experiments.

Fig. 4a shows an example of a typical PPG signal recorded from the earlobe with the earring sensor in comparison to an ECG signal recorded simultaneously while the participant was standing still. It is evident from the figure that for every QRS complex, there is a corresponding peak of the peripheral pulse that is clearly distinguishable in the PPG waveform. There is a slight lag between the R wave and the peak of the PPG waveform due to the pulse transit time. A dicrotic notch can also be observed in several PPG waveforms. The differences between heart rate measurements recorded by the earring sensor and ECG (expressed as percentage of average of both measurements) during standing from 14 participants (218 pairs of 15 s epoch measurements) are displayed in a Bland-Altman plot (Fig. 4b). The limits of agreement (±1.96SD) reflect where 95% of all differences between measurements are expected to lie. During standing at rest, the mean bias $\bar{d}$ was 0.62% with 95% limits of agreement of -8.23 to 9.46% and the mean absolute bias $|\bar{d}|$ was 2.74%. The correlation coefficient r between both sets of measurements was 0.97 ($p < 0.001$).

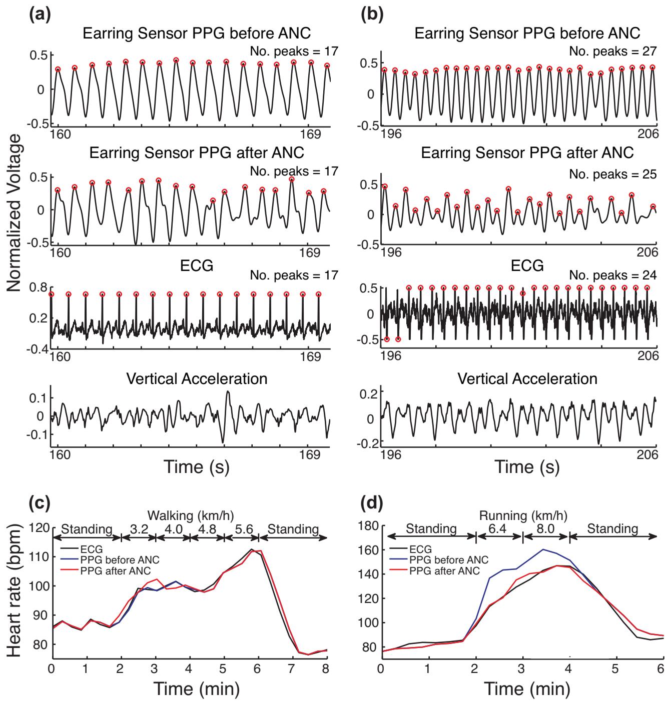

Fig. 5. Comparison of 10 s earring sensor PPG waveforms before and after ANC using corresponding vertical acceleration signal as noise reference during (a) walking and (b) running. Red circles indicate detected peaks. Heart rate curves measured by earring sensor before (blue line) and after ANC (red line), as well as by reference ECG (black line) during (c) walking and (d) running. ANC was not applied during standing (red and blue lines overlap).

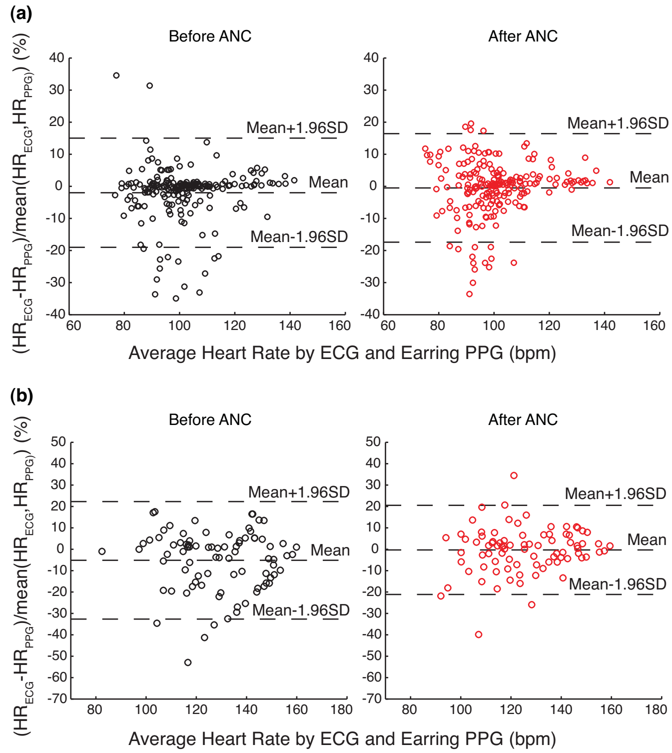

Fig. 6. Bland-Altman plots demonstrating the agreement between 15 s epoch heart rate measurements from the earring sensor and ECG before (black circles) and after (red circles) ANC during (a) walking (a total of 202 measurement pairs from 14 subjects) and (b) running (a total of 84 measurement pairs from 12 subjects). The lines represent the mean and 95% limits of agreement.

B. *Measurements During Walking Show High Agreement Before and After ANC*

The performance of our system was also tested in the presence of moderate motion during walking at speeds of 3.2-5.6 km/h. Fig. 5a illustrates the effect of ANC on the PPG waveform during walking obtained from the earring sensor. Even before ANC, the PPG signal is in good accord with the ECG signal with an equal number of peaks within the 10 s time window displayed. In this case, ANC changed the shape of the waveform and some of the peak arrival times, but the number of peaks remained the same. As a result, the average heart rate calculation didn't change significantly as presented in Fig. 5c. Both before and after ANC heart rate curves closely matched the ECG-derived heart rate curve throughout the experiment with the measurements before ANC providing a slightly better match. When the agreement between 202 pairs of measurements from 14 participants was tested by Bland-Altman analysis (Fig. 6a), $\bar{d}$ was -1.98% with 95% limits of agreement -19.00 to 15.04% before ANC. After applying ANC, $\bar{d}$ was lowered to -0.49% with 95% limits of agreement -17.39 to 16.42%. However, the $|\bar{d}|$ increased slightly from 4.79% to 5.92% after ANC, which is consistent with the wider spread of points within the limits of agreement after ANC. Despite the larger limits of agreement compared to standing, the distribution of points was mainly concentrated near zero in both cases. Both scenarios also yielded a high correlation coefficient *r* between measurements of 0.82 ($p < 0.001$).

C. *ANC Significantly Improves Performance of Earring Sensor During Running*

To evaluate the effect of vigorous activity on the performance of our system, we tested it during running experiments at speeds of 6.4-8.0 km/h. The ability of ANC to reduce the effect of motion artifacts during running is illustrated in Fig 5b. Before ANC, the number of peaks within the 10 s window shown was overestimated by three compared to the number of QRS complexes. However, after ANC the PPG waveform was altered such that two extra beats were removed (the first failed the time threshold and the other failed the amplitude threshold). In this example, while the average heart rate measurements were approximately 20 bpm higher throughout the running session before ANC, after ANC the measurements were much closer (within 6 bpm) to those obtained with ECG (Fig. 5d). From the Bland-Altman analysis of 84 pairs of measurements from 12 participants, we see a significant difference in the distribution of points before and after ANC (Fig. 6b). Before ANC, $\bar{d}$ was -5.17% with 95% limits of agreement -32.64 to 22.29%. After applying ANC, the points were distributed closer to zero and $\bar{d}$ was reduced to -0.32% with 95% limits of agreement -21.15 to 20.52%. ANC also reduced $|\bar{d}|$ from 10.77% to 7.68%. In addition, the correlation coefficient between both sets of measurements increased from 0.57 to 0.75 after ANC ($p < 0.001$ for both).

TABLE 2
DESCRIPTIVE STATISTICS OF HEART RATE MEASUREMENTS BY EARRING SENSOR PPG AND ECG

Statistic	Standing (at rest)	Walking (before ANC)	Walking (after ANC)	Running (before ANC)	Running (after ANC)
No. of measure-ment pairs	218	202	202	84	84
Mean bias (%)	0.62	-1.98	-0.49	-5.17	-0.32
Mean absolute bias (%)	2.74	4.79	5.92	10.77	7.68
SD of bias (%)	4.51	8.68	8.63	14.01	10.63
Upper limit (%)	9.46	15.04	16.42	22.29	20.52
Lower limit (%)	-8.23	-19.00	-17.39	-32.64	-21.15
Correlation coefficient	0.97*	0.82*	0.82*	0.57*	0.76*

Measurements based on 15 s epochs from 12-14 participants (a total of 84-218 measurement pairs). ANC performed with 7th order FIR filter using the LMS algorithm with a step size of 0.2. Walking speed tested from 3.2-5.6 km/h. Running speed tested from 6.4-8.0 km/h. Upper and lower limit refer to 95% limits of agreement.

*Indicates significance at $p < 0.001$

V. DISCUSSION

Intelligent design of sensor attachment and use of advanced signal processing methods are required for the development of wearable biosensors capable of providing accurate measurements during daily activities. Wearable devices that are compact, robust and comfortable will enable widespread use in extending the care and support of emergency operators. Given that the proposed device was designed to resemble a regular communication earpiece that is commonly used by emergency operators, this approach is favorable for unobtrusive and discreet health monitoring. The new device was found to be comfortable by the 14 wearers who participated in our activity experiments.

Critical performance evaluation is very important for the validation of any wearable biosensor and this is an aspect of our study that is lacking in previous works on ear-worn PPG sensors (Table 1b). The descriptive statistics for critical evaluation of the proposed system compared to standard ECG heart rate measurements under conditions at rest (standing), during moderate (walking) and vigorous activity (running) are summarized in Table 2. Overall, our device showed very high agreement ($\bar{d} = 0.62 \pm 4.51\%$) with ECG measurements during standing and relatively precise measurements with the use of ANC during activities such as walking ($\bar{d} = -0.49 \pm 8.63\%$) and running ($\bar{d} = -0.32 \pm 10.63\%$). In both the walking and running experiments, ANC reduced the mean bias and standard deviation as well as increased the level of correlation. No sensor is perfectly immune to all motion artifacts; thus, it is important to characterize the kinds of variations that may happen during natural activities. The widening 95% limits of agreement during walking (-17.39 to 16.42%) and running (-21.15 to 20.52%) may partially be due to the variability in terms of the snugness of the wireless earpiece among the participants. A poorly fitted earpiece would introduce more sources of artifacts and these disturbances would become more apparent with increasing levels of vigorous activities. Having a range of earhook sizes available to ensure the best fit for each user would help minimize this variation. Although we chose an averaging window of 15 s, using a longer epoch such as one covering at least 60 beats could improve the confidence in a single timing measurement [2] extracted from the PPG waveform at the expense of a longer measurement lag. Ultimately, this is a tradeoff between higher accuracy and faster measurement updates; the optimum choice depends on the particular application.

Another source of variation in the effectiveness of ANC in heart rate measurements is the positioning of the sensor and its ability to effectively model the induced motion artifacts. In our studies we chose to use the acceleration along the longitudinal (vertical) axis of the trunk as the reference noise signal because it provides the highest correlation during jogging/running and has been shown to provide a better motion reference than the summation of all three axes [30]. Nonetheless, using all three accelerometer signals would be advantageous if the sensor was misaligned during motion. Although the walking posture of the trunk is vertical in most individuals, any tilt away from this axis would result in attenuation of the signal and reduce the validity of the vertical axis as the noise reference signal. Furthermore, there exists a higher degree of variation in the degree to which participants would lean forward during running at increasing speeds [31]. By combining information from all three axes of the accelerometer or adaptively selecting the axis with the highest correlation to the current corrupted signal, it may be possible to improve on the accuracy of the motion reference signal. In many cases of walking, motion artifacts did not corrupt the original raw signal obtained by our earring sensor and none of the three accelerometer signals would significantly improve performance. In situations like this whereby physical activity (other examples include mild head shaking/nodding etc.) does not affect the earring sensor's reading, it is better not to apply ANC. Thus, context-awareness (interpretation of physical activity or physiological condition under which the PPG waveform is measured) is needed beyond simple correlation analysis for better performance.

The version of ANC implemented in this first prototype of the novel earring PPG system used the classic algorithm. The effectiveness of this form of ANC can be further improved simply by increasing the filter order used to implement the adaptive algorithm [12], but at the cost of longer computation time which is undesirable for real-time parameter estimations. There are also many newer variations on ANC that may be promising; for example, one might utilize the Laguerre model to approximate the PPG response to acceleration, which has been reported to improve error reduction over an FIR filter [32]. An FIR model always has high variances, as the relatively wide limits of agreement in our results during running also indicate, but the Laguerre model has much lower variance due to fewer tuning parameters [11]. There are two choices available for implementing real-time ANC. The first would be to perform all the computation on the DSC. To avoid the overflow problem during multiply-accumulate (MAC) operations, fractional arithmetic is implemented and a 17-bit × 17-bit hardware multiplier allows the dsPIC to multiply two 16-bit values together. The ADC resolution is 12-bits which allows for four additional bits to prevent round-off errors. Furthermore, since our ANC model only uses a 7th order filter, the LMS algorithm would only require seven MAC operations; thus round-off errors would be negligible. If one desired to employ more sophisticated noise-cancellation algorithms that were beyond the computational capability of the dsPIC, performing real-time ANC on the receiving PC is another option.

We have described, demonstrated, and evaluated an innovative design approach for wearable PPG sensing on the earlobe that is motion tolerable during physical activities important in the course of emergency operations such as running. To the best of our knowledge, this is the first demonstration of a fully integrated, self-contained ear-worn design that can be conveniently incorporated into equipment already worn routinely by many emergency operators. Although this paper focused on validating the proposed device in terms of heart rate estimates, many other important physiological parameters can be extracted from the PPG signal such as oxygen saturation [33], respiratory rate [34] and autonomic function [35]. Furthermore, the embedded three-axis accelerometer can also be utilized for activity classification and metabolic energy expenditure estimation [36-38]. The proposed device serves as a new wearable platform that enables these clinical variables to be measured in a comfortable, discreet, and unobtrusive manner using an earring and earpiece form factor already proven to be acceptable to a large population of wearers. Adding these additional physiological parameter extraction capabilities will be the subject of future work.

Acknowledgment

The authors thank J. Lee, A. D. Goessling, Y. K. Cheung and S. Goyal for their assistance and valuable feedback, K. H. Kim for actively recruiting participants for this study and Thought Technologies for generously donating the Flexcomp Infiniti system.

References

[1] P. Bonato, "Wearable sensors/systems and their impact on biomedical engineering," *IEEE Eng Med Biol Mag,* vol. 22, pp. 18-20, May-Jun 2003.

[2] J. Allen, "Photoplethysmography and its application in clinical physiological measurement," *Physiol Meas,* vol. 28, pp. R1-39, Mar 2007.

[3] S. Vogel, M. Hulsbusch, D. Starke, and S. Leonhardt, "A system for assessing motion artifacts in the signal of a micro-optic in-ear vital signs sensor," in *Proc. 30th Annu. Int. Conf. IEEE Engineering in Medicine and Biology Society*, Vancouver, Canada, 2008, pp. 510-3.

[4] S. Rhee, B. H. Yang, and H. H. Asada, "Artifact-resistant power-efficient design of finger-ring plethysmographic sensors," *IEEE Trans Biomed Eng,* vol. 48, pp. 795-805, Jul 2001.

[5] P. Renevey, R. Vetter, J. Krauss, P. Celka, and Y. Depeursinge, "Wrist-located pulse detection using IR signals, activity and nonlinear artifact cancellation," in *Proc. 23rd Annu. Int. Conf. IEEE Engineering in Medicine and Biology Society*, Istanbul, Turkey, 2001, p. 3030.

[6] S. Lee, B. L. Ibey, W. Xu, M. A. Wilson, M. N. Ericson, and G. L. Cote, "Processing of pulse oximeter data using discrete wavelet analysis," *IEEE Trans Biomed Eng,* vol. 52, pp. 1350-2, Jul 2005.

[7] Y. S. Yan, C. C. Poon, and Y. T. Zhang, "Reduction of motion artifact in pulse oximetry by smoothed pseudo Wigner-Ville distribution," *J Neuroeng Rehabil,* vol. 2, p. 3, Mar 1 2005.

[8] Y. S. Yan and Y. T. Zhang, "An efficient motion-resistant method for wearable pulse oximeter," *IEEE Trans Inf Technol Biomed,* vol. 12, pp. 399-405, May 2008.

[9] M. J. Hayes and P. R. Smith, "Artifact reduction in photoplethysmography," *Appl Opt,* vol. 37, pp. 7437-46, Nov 1 1998.

[10] H. H. Asada, H. Jiang, and P. Gibbs, "Active noise cancellation using MEMS accelerometers for motion-tolerant wearable bio-sensors," *Conf Proc IEEE Eng Med Biol Soc,* vol. 1, pp. 2157-2160, 2004.

[11] L. B. Wood and H. Asada, "Low variance adaptive filter for cancelling motion artifact in wearable photoplethysmogram sensor signals," *Conf Proc IEEE Eng Med Biol Soc,* vol. 2007, pp. 652-5, 2007.

[12] G. Comtois, Y. Mendelson, and P. Ramuka, "A comparative evaluation of adaptive noise cancellation algorithms for minimizing motion artifacts in a forehead-mounted wearable pulse oximeter," *Conf Proc IEEE Eng Med Biol Soc,* vol. 2007, pp. 1528-31, 2007.

[13] S. H. Kim, D. W. Ryoo, and C. Bae, "Adaptive noise cancellation using accelerometers for the PPG signal from forehead," *Conf Proc IEEE Eng Med Biol Soc,* vol. 2007, pp. 2564-7, 2007.

[14] H. Han, Y. Lee, and J. Kim, "Development of a wearable health monitoring device with motion artifact reduced algorithm," in *Proc. Int. Conf. Control, Automation and Sys.*, Seoul, Korea, 2007.

[15] B. Widrow, J. R. Glover, M. J.M., J. Kaunitz, W. C.S., R. H. Hearn, Z. J.R., E. D. Dong, and R. Goodlin, "Adaptive Noise Cancelling: Principles and Applications," *Proceedings of the IEEE,* vol. 63, pp. 1692-1716, 1975.

[16] Y. Mendelson, R. J. Duckworth, and G. Comtois, "A wearable reflectance pulse oximeter for remote physiological monitoring," in *Proc. 28th Annu. Int. Conf. IEEE Engineering in Medicine and Biology Society*, New York, USA, 2006, p. 912.

[17] P. Celka, C. Verjus, R. Vetter, P. Renevey, and V. Neuman, "Motion resistant earphone located infrared based heart rate measurement device," in *Proc. 2nd Int. Conf. Biomedical Engineering*, Innsbruck, Austria, 2004, p. 582.

[18] L. Wang, B. Lo, and G. Z. Yang, "Multichannel reflective PPG earpiece sensor with passive motion cancellation," *IEEE Trans Biomed Circuits Syst,* vol. 1, pp. 235-241, 2007.

[19] A. B. Hertzman, "The blood supple of various skin areas as estimated by the photoelectric plethysmograph," *Am J Physiol,* vol. 124, pp. 328-340, 1938.

[20] R. M. Stern, "Ear lobe photoplethysmography," *Psychophysiology,* vol. 11, pp. 73-5, Jan 1974.

[21] H. H. Asada, P. Shaltis, A. Reisner, S. Rhee, and R. C. Hutchinson, "Mobile monitoring with wearable photoplethysmographic biosensors," *IEEE Eng Med Biol Mag,* vol. 22, pp. 28-40, May-Jun 2003.

[22] K. Shin, Y. Kim, S. Bae, K. Park, and S. Kim, "A novel headset with a transmissive PPG sensor for heart rate measurement," in *Proc. 13th Int. Conf. on Biomed. Eng.*, Singapore, 2009.

[23] S. Vogel, M. Hulsbusch, D. Starke, and S. Leonhardt, "In-ear heart rate monitoring using a micro-optic reflective sensor," in *Proc. 30th Annu. Int. Conf. IEEE Engineering in Medicine and Biology Society*, Lyon, France, 2007, p. 1375.

[24] T. Wartzek, S. Vogel, T. Hennig, O. Brodersen, M. Hulsbusch, M. Herzog, and S. Leonhardt, "Analysis of heart rate variability with an in-ear micro-optic sensor in view of motion artifacts," in *Proc. Sixth Int. Workshop on Wearable and Implantable Body Sensor Networks*, Berkeley, CA, 2009.

[25] C. Z. Wang and Y. P. Zheng, "Home-telecare of the elderly living alone using an new designed ear-wearable sensor," in *Proc. 5th Int. Workshop on Wearable and Implantable Body Sensor Networks*, Hong Kong, China, 2008.

[26] J. A. C. Patterson, D. G. McIlwraith, and G. Z. Yang, "A flexible, low noise reflective PPG sensor platform for ear-worn heart rate monitoring," in *Proc. Sixth Int. Workshop on Wearable and Implantable Body Sensor Networks*, Berkeley, CA, 2009.

[27] J. M. Bland and D. G. Altman, "Statistical methods for assessing agreement between two methods of clinical measurement," *Lancet,* vol. 1, pp. 307-10, Feb 8 1986.

[28] L. B. Wood, "Motion artifact reduction for wearable photoplethysmogram sensors using micro accelerometers and Laguerre series adaptive filters," S.M. thesis, Massachusetts Institute of Technology, Cambridge, MA, USA, 2004.
[29] Q. Zhang, A. I. Manriquez, C. Medigue, Y. Papelier, and M. Sorine, "An algorithm for robust and efficient location of T-wave ends in electrocardiograms," *IEEE Trans Biomed Eng,* vol. 53, pp. 2544-52, Dec 2006.
[30] G. Comtois and Y. Mendelson, "A noise reference input to an adaptive filter algorithm for signal processing in a wearable pulse oximeter," in *Proc. IEEE 33rd Ann. Northeast Bioeng. Conf.*, 2007.
[31] S. Brage, N. Brage, P. W. Franks, U. Ekelund, and N. J. Wareham, "Reliability and validity of the combined heart rate and movement sensor Actiheart," *Eur J Clin Nutr*, vol. 59, pp. 561-70, Apr 2005.
[32] H. H. Asada, H. Jiang, and P. Gibbs, "Active motion artifact reduction for wearable sensors using Laguerre expansion and signal separation," *Conf Proc IEEE Eng Med Biol Soc,* vol. 1, pp. 3571-3574, 2005.
[33] C. M. Alexander, L. E. Teller, and J. B. Gross, "Principles of pulse oximetry: theoretical and practical considerations," *Anesth Analg,* vol. 68, pp. 368-76, Mar 1989.
[34] A. Johansson and P. A. Oberg, "Estimation of respiratory volumes from the photoplethysmographic signal. Part I: Experimental results," *Med Biol Eng Comput,* vol. 37, pp. 42-7, Jan 1999.
[35] W. B. Murray and P. A. Foster, "The peripheral pulse wave: information overlooked," *J Clin Monit,* vol. 12, pp. 365-77, Sep 1996.
[36] D. M. Karantonis, M. R. Narayanan, M. Mathie, N. H. Lovell, and B. G. Celler, "Implementation of a real-time human movement classifier using a triaxial accelerometer for ambulatory monitoring," *IEEE Trans Inf Technol Biomed,* vol. 10, pp. 156-67, Jan 2006.
[37] M. Ermes, J. Parkka, J. Mantyjarvi, and I. Korhonen, "Detection of daily activities and sports with wearable sensors in controlled and uncontrolled conditions," *IEEE Trans Inf Technol Biomed,* vol. 12, pp. 20-6, Jan 2008.
[38] J. Parkka, M. Ermes, P. Korpipaa, J. Mantyjarvi, J. Peltola, and I. Korhonen, "Activity classification using realistic data from wearable sensors," *IEEE Trans Inf Technol Biomed,* vol. 10, pp. 119-28, Jan 2006.

Ming-Zher Poh (S'09) received the B.Sc. (Hons.) degree (*magna cum laude*) in electrical and computer engineering from Cornell University, Ithaca, NY in 2005, and the S.M. degree in electrical engineering from the Massachusetts Institute of Technology (MIT), Cambridge, MA in 2007.

He is currently pursuing a Ph.D. degree in electrical and medical engineering at the Harvard-MIT Division of Health Sciences and Technology (HST). His work experience includes developing microfluidic biochips at the MGH Center for Engineering in Medicine and optimizing delivery of nanoparticles to tumors at the MGH Department of Radiation Oncology. Since 2008, he has been with the Affective Computing Group at the MIT Media Lab. His current research interests include neurophysiology, wearable biosensors and assistive technologies for neurological disorders such as epilepsy and autism.

Mr. Poh is also a student member of Tau Beta Pi and an associate member of Sigma Xi.

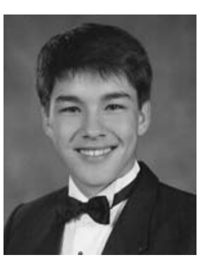

Nicholas C. Swenson is an undergraduate student pursuing a B.Sc. degree in biomedical engineering at the Massachusetts Institute of Technology (MIT), Cambridge, MA.

He is currently a member of the Affective Computing Group at the MIT Media Lab. He has done research using hyperbaric therapy on wounds in diabetic patients at the Riverside Hospital in Newport News, VA in 2006-2007. He has also conducted research at the Mary Immaculate Hospital in Grafton, VA on the venous blood flow during different total hip arthroplasties in 2007-2008.

Rosalind W. Picard (M'81–SM'00–F'05) earned a bachelors in electrical engineering with highest honors from the Georgia Institute of Technology in Atlanta, GA in 1984, and S.M. and Sc.D. degrees in electrical engineering and computer science from MIT in Cambridge, MA, in 1986 and in 1991.

She is Professor of Media Arts and Sciences at the MIT Media Lab, founder and director of the Affective Computing Group, and leader of a new Autism and Communication Technology Initiative at MIT in Cambridge, MA. Author of around two hundred scientific articles, she is best known for pioneering work in image and video content based retrieval (the original Photobook system), for developing texture models and machine learning for their combination (Society of Models) and for her book Affective Computing (MIT Press, 1997), which helped launch a field by that name. Her work experience includes Member of the Technical Staff at AT&T Bell Labs in Holmdel, NJ (1984-1987), internships at Hewlett Packard, IBM, and Scientific Atlanta, and consulting at a variety of companies including Apple, IRobot, BT, and Motorola. Current research interests focus on the development of technology to help people comfortably and respectfully measure and communicate affective information, as well as on the development of models of affect that improve decision-making and learning.

Dr. Picard is also a member of the ACM and a recipient of a best paper prize from IEEE ICALT in 2001.